Published in final edited form as:
J Magn Reson Imaging. 2008 April ; 27(4): 732–736.

MR Analysis of Regional Brain Volume in Adolescent Idiopathic Scoliosis: Neurological Manifestation of a Systemic Disease

Tianming Liu, PhD[1], **Winnie C.W. Chu, MD**[2,*], **Geoffrey Young, MD**[1], **Kaiming Li, MS**[1,3], **Benson H.Y. Yeung, PhD**[4], **Lei Guo, PhD**[3], **Gene C.W. Man, BSc**[4], **Wynnie W.M. Lam, MD**[2], **Stephen T.C. Wong, PhD**[1], and **Jack C.Y. Cheng, MD**[4]

1*Functional and Molecular Imaging Center, Department of Radiology, Brigham and Women's Hospital, Harvard Medical School, Boston, Massachusetts.*

2*Departments of Diagnostic Radiology and Organ Imaging, The Chinese University of Hong Kong, Hong Kong.*

3*School of Automation, Northwestern Polytechnic University, Xi'an, PR China.*

4*Departments of Orthopaedics and Traumatology, The Chinese University of Hong Kong, Hong Kong.*

Abstract

Purpose—To investigate whether regional brain volumes in adolescent idiopathic scoliosis (AIS) patients differ from matched control subjects as AIS subjects are reported to have poor performance on combined visual and proprioceptive testing and impaired postural balance in previous studies.

Materials and Methods—Twenty AIS female patients with typical right-convex thoracic curve (age range,11−18 years; mean, 14.1 years) and 26 female controls (mean age, 14.8 years) underwent three-dimensional magnetization prepared rapid acquisition gradient echo (3D-MPRAGE) MR imaging. Volumes of 99 preselected neuroanatomical regions were compared by statistical parametric mapping and atlas-based hybrid warping.

Results—Analysis of variance statistics revealed significant mean volumetric differences in 22 brain regions between AIS and controls. Ten regions were larger in AIS including the left frontal gyri and white matter in left frontal, parietal, and temporal regions, corpus callosum and brainstem. Twelve regions were smaller in AIS, including right-sided descending white matter tracts (anterior and posterior limbs of the right internal capsule and the cerebral peduncle) and deep nucleus (caudate), bilateral perirhinal cortices, left hippocampus and amygdala, bilateral precuneus gyri, and left middle and inferior occipital gyri.

Conclusion—Regional brain volume difference in AIS subjects may help to explain neurological abnormalities in this group.

Keywords

adolescent idiopathic scoliosis; magnetic resonance; brain morphometry

ADOLESCENT IDIOPATHIC SCOLIOSIS (AIS) is a complex three-dimensional spine deformity that most commonly occurs in adolescent girls during the pubertal period. The prevalence in Hong Kong is nearly 4%. Untreated or improperly treated scoliotic deformity may deteriorate progressively leading to significant cosmetic problems and functional

*Address reprint requests to: W.C.W.C., The Chinese University of Hong Kong, Prince of Wales Hospital, HKSAR, China. E-mail: address: winnie@med.cuhk.edu.hk.

disabilities. In severe cases, increased mortality rate can result from the associated early onset cardiopulmonary failure.

No preventive treatment for idiopathic scoliosis is currently available, in part because the etiology of AIS is not well understood. Current treatments are pragmatic and involve long-term bracing (1,2) or invasive major surgery with instrumentation and spinal fusion (3), which is associated with many potential complications (4).

Observation of subclinical neurological abnormalities in AIS patients has led to the proposal of a neurodevelopmental etiologic model for AIS (5–12). Longer latency in somatosensory-evoked potential (SSEP) has been demonstrated by Cheng et al (13,14) and Hausmann et al (15), suggesting disturbed somatosensory function and impaired balance control (16,17) in AIS subjects. As low-lying cerebellar tonsils have been documented in AIS patients (18–20), we hypothesize that other intracerebral structural abnormalities might be present that could contribute to inappropriate postural adjustment during the growth spurt and so explain the progressive spinal deformity observed in the early adolescence of AIS subjects.

In the present study, regional brain volumes were assessed by three-dimensional (3D) MR technique. A whole brain parcellation method based on a hybrid volumetric and surface warping algorithm (21,22) was used to compare the morphologic brain data sets from AIS subjects with those acquired from age and sex-matched normal controls.

MATERIALS AND METHODS

Subjects

Forty-six right-handed Chinese adolescent girls 11 to 18 years of age were prospectively recruited in this study. Among the subjects, there were 20 AIS girls (mean age, 14.1 years) with moderate to severe right-thoracic curve (the most prevalent curve type in AIS), consecutively recruited from the outpatient scoliosis clinic. Twenty-six healthy volunteer controls (all girls; mean age, 14.8 years) were invited to participate in the study from local schools. Patients with any history of head injury, headache, back injury, weakness or numbness in one or more limbs, urinary incontinence, nocturnal enuresis, or any space-occupying lesion found on screening MR imaging were excluded. There was no significant statistically difference in age between the two groups. In AIS patients, the Cobbs angles measured by standard long film ranged from 37° to 68° (mean, 53°). Standing height as measured on long film was not significantly different between patient and control groups, after standard correction in the AIS group. All subjects were found to be neurologically normal on detailed neurological examination. The presence of mild scoliotic curve were excluded in all controls by Adams forward bending test by experienced orthopedic surgeons. The local ethics committee of the institution approved the study, and informed written consent was obtained from all subjects and their parents.

Magnetic Resonance Imaging

MRI of the brain was performed in all subjects using 1.5-T MR Scanner (Sonata, Siemens, Erlanger, Germany) using a quadrature head coil. High spatial resolution anatomic imaging was performed with a magnetization prepared rapid acquisition gradient echo (MPRAGE) sequence with repetition time (TR) = 2070 ms, echo time (TE) = 3.93 ms, inversion time (TI) = 1110 ms, flip angle = 15 degrees, field of view (FOV) = 230 mm, slice thickness = 0.9 mm, no gap, matrix = 256 × 256 × 128, number of excitation = 1). The sequence yielded high quality isotropic images with the voxel size of 0.9 × 0.9 × 0.9 mm. The scanning time for each subject was 8.5 min.

Region-Based Morphometry Analysis

We used published methods (21) for preprocessing and brain tissue segmentation. Afterward, a previously validated and reported hybrid volumetric and surface warping method (21,22) was used to automatically parcellate the structural brain MR image into 99 neuroanatomic regions. In the first step of the hybrid method, a feature-based volumetric registration algorithm HAMMER (23) was used to warp a model cortical surface to the individual's space. This volumetric registration algorithm had relatively high accuracy in matching cortical gyrations and greatly reduced the variation between the model and individual brains, resulting in a good initialization for the subsequent surface warping. In the second step, a surface registration algorithm based on the matching of geometric attribute vectors was used to further warp the model surface to the subject. It is well known that there is tremendous morphological variation in the human cortex (24), which could introduce many local minima during the minimization of the energy function of registration. To address this problem, an adaptive deformation strategy was applied in the surface registration algorithm to reduce the chances of being trapped of local minima. In the hybrid warping algorithm (21), it was guaranteed that both volumetric and surface warping steps preserved topology, thus the finally warped model surface also preserved its topology.

After the high-dimensional hybrid registration and atlas-based warping, the subject brain image was segmented into 99 neuroanatomic regions by mapping the anatomic labels in the atlas to the subject. In parallel to this process, an automatic tissue segmentation method described in Zhang et al (25) was applied to the subject's structural MR data and the resulting tissue maps were used to mask the automatically labeled structural MR images, generating labeled regional maps(22). Figure 1 summarizes the whole procedure of automatic brain parcellation using one randomly selected AIS patient's brain MR image. As shown in Figure 1, the hybrid registration algorithm provided atlas-based anatomic segmentation of the subject's volumetric image, and the tissue segmentation map provided local adjustment of the automated parcellation. After the anatomic segmentation, each region volume was normalized by the intracranial volume of the subject's brain, as it was shown that this normalization procedure reduced inter-individual variations (26). The intracranial volume was derived using the automated segmentation process of 3D subject brain (22).

Statistical Analysis

Normalized regional brain volume differences between AIS group and normal controls were analyzed by analysis of variance using Statistical Package for Social Science (SPSS) for Windows (SPSS Version 14, Chicago, IL). Significance threshold was set at $P < 0.01$.

RESULTS

Normalized mean brain volumes in AIS subjects were significantly different ($P < 0.01$) from matched controls in 22 of 99 anatomical regions. The normalized mean regional brain volume ratios in the above areas for both AIS subjects and controls and the *P* values are summarized in Table 1. The normalized regional volumetric ratios of the left superior frontal gyrus, left medial frontal gyrus, left lateral fronto-orbital gyrus, left postcentral gyrus, left thalamus, left frontal lobe, parietal lobe, and temporal lobe white matter were shown to be significantly larger in AIS subjects than in controls. Also, midline structures including the corpus callosum and brainstem were shown to be larger in AIS subjects. The anterior and posterior limbs of right internal capsule, right cerebral peduncle, right caudate nucleus, left middle occipital gyrus, left inferior occipital gyrus, left amygdale, left hippocampus, right temporal pole, and bilateral precuneus and perirhinal cortices were found to be significantly smaller in AIS subjects.

DISCUSSION

It has been hypothesized that the etiology of AIS could involve subclinical neuromuscular dysfunction, in which occult neurological disorder during growth could present as deformity in the multisegmented spine. AIS patients have been demonstrated to respond poorly on combined tests for visual and proprioceptive function when compared with controls (12), impaired spatial orientation (27), poor postural control (5–7,17,28), abnormal nystagmus response to caloric testing (8,9,29), asymmetric otolith vestibulo-ocular responses (30), and abnormal sway patterns using stabilometry. Abdominal reflexes were found to be asymmetrical by another study (11). One study has reported an increase in SSEP latencies corrected for body height in 68 of 100 AIS patients (15). Our previous research findings have suggested that the site of SSEP abnormality in AIS originated from a level above the cervical spine (31) and likely to be linked to disturbances along the spinocortical pathway.

Lowe et al (32) proposed that pontine and hindbrain regions are the most likely sites of primary pathology. Herman et al (27) suggested a higher level central nervous system disturbance producing visuospatial perceptual impairment, motor adaptation, and learning deficits leading to a faulty recalibration of proprioceptive signals from axial musculature. There has been much speculation about possible sites of neurological abnormality in AIS, but to date, little data have been available to test these hypotheses. Recent advances in MR imaging and computational image analysis allowing quantification of volumes of different brain regions may provide an opportunity to address these hypotheses.

In this pilot study, we have demonstrated the feasibility of applying morphometric method to the study of brain regions in AIS and found significant regional anatomical differences between AIS subjects and matched controls. Several regions of the left brain hemisphere were enlarged in right convex AIS subjects including superior frontal, medial frontal, and lateral orbitofrontal gyri. In addition to enlargement of these left hemispheric cortical gyri, white matter volumes in the left frontal, parietal, and temporal lobes were enlarged. Conversely, these right convex AIS patients were found to have relative hypoplasia of structures transmitting the right-sided descending white matter tracts, including the anterior and posterior limbs of the right internal capsule and the cerebral peduncle. Similarly, the deep nuclei were smaller in AIS subjects.

Previous studies have shown left–right asymmetry in the upper limbs (33) and lower limbs (34) in AIS subjects. Our findings of corresponding brain asymmetry suggest a possible neuroanatomic substrate for this somatic asymmetry. The finding of asymmetric size in the deep nuclei is especially intriguing in this regard, given the function of these nuclei to modulate tonic and task-dependent activation of the efferent motor pathways (35). Because all AIS subjects in this study had typical right convex thoracic curvature, additional investigation will be needed to see whether this pattern is reversed in AIS patients with left convex scoliotic curvature.

Bilateral perirhinal cortices on the ventral surface of temporal lobes were also found to be significantly different between AIS subjects and normal controls. As perirhinal cortex has recently been recognized to play a critical role in object recognition, object identification, and perception (36), these changes might be related to the impairment of visual and spatial perception, motor adaptation (27,29), and proprioception (12) reported in AIS. The right temporal pole, left hippocampus, and left amygdala were also found to be different. Whether this finding is independent of the perirhinal cortex finding or is related to it on the basis of the interaction between these areas for information storage and object knowledge may be worthy of further investigation (36).

The thickness of the corpus callosum, the principle commissural fiber bundle connecting left and right hemispheres, was found to be significantly larger in AIS subjects. This is an intriguing

finding in a disorder of somatic symmetry, especially in light of the neuroanatomic asymmetry demonstrated above. Abnormal function of the corpus callosum might lead to poor coordination of the left and right body and might contribute to impaired postural balance in AIS subjects. This possibility raises the interesting question of whether the morphologic hypertrophy of the corpus callosum is a primary causative feature of the suspected bilateral motor discoordination or results from a compensatory response to that imbalance. This may be an important question to address in further animal and human studies.

In our analysis, the brainstem proved to be larger in AIS subjects. The brainstem has been previously postulated to be a primary site of pathology in AIS subjects (32). Prior evidence for this hypothesis includes rat studies showing that scoliosis can be induced by creating microscopic lesions in the pons and periaqueductal gray matter by electrocoagulation.(37). In addition, reports of a high prevalence of symmetrical horizontal and lateral gaze palsy in patients with idiopathic scoliosis (38), and abnormal nystagmus response to calorie testing (10) suggest that an abnormality of the paramedian pontine reticular formation linking preocular motor nuclei and vestibular nuclei may be present in many AIS patients.

Bilateral precuneus, left middle occipital gyrus, and left inferior occipital gyrus were found to be significantly smaller in AIS subjects. These areas are closely related to visual cortex and thus might be related to visual comprehension deficits and involuntary eye movements reported in AIS subjects (9,10).

Although some of the regional differences found in this study are of uncertain significance, the majority seem to be related either directly to corticospinal efferent motor control, or to coordination of motor function and its modulation in response to visual and somatic inputs. Specific asymmetries were detected that support the existence of an anatomic and likely functional imbalance of the descending corticospinal tracts. Brain regions modulating motor function and coordination that seem to be involved include the deep nuclei, pre-motor cortices, midbrain structures, and regions of the temporal and occipital lobes involved in visual and spatial processing. It is reassuring that these anatomic findings correlate well with the subclinical somatosensory dysfunction documented in AIS patients. Most importantly, the finding of asymmetry of callosal commissural fibers generates the hypothesis—testable in animal models—that a primary deficit in interhemispheric coordination could play a primary role in the pathophysiology of the disorder.

In this study, the region-based morphometry analysis method based on automated segmentation of the whole brain was applied to study the morphological difference between AIS patients and normal controls. The rationale is that the region-based morphometry analysis method and nonlinear support vector machine method (39) combine the advantages of region of interest (ROI) analysis and voxel-based morphometry (40), as they do not require a priori hypothesis and provide automation (as voxel-based morphometry), as well as having more interpretable results (as ROI analysis).

This pilot study only reported structural changes based on conventional MRI. To substantiate our hypothesis of functional impairment of somatic motor control and coordination in AIS subjects, functional MRI (fMRI) studies would be the next step to explore the possible deficit in the spatial and visual processing and, hence, motor modulation in AIS subjects. A full diffusion tensor imaging study, including tractography, which explores the integrity of white matter fibers (41–43), may also be of value for further understanding the white matter pathways in AIS.

In summary, this small preliminary study has documented the presence of neuroanatomic asymmetries in regions of the brain functionally related to somatic motor control and coordination. This finding provides the feasibility and potential interest of quantification of

regional neuroanatomy in AIS patients and supports the hypothesis that spine deformity in AIS may represent the somatic sequelae of a neuromuscular imbalance or dyscoordination originating in the brain. Larger scale human MRI morphometry studies will be required to confirm our findings, but the preliminary results suggest intriguing and potentially testable pathophysiologic hypotheses.

Acknowledgements

Contract grant sponsor: Hong Kong Research Grant Council; Contract grant number: CUHK 4506/05M; Contract grant sponsor: the Foundation Yves Cotrel de l'Institut de France; Contract grant sponsor: the Harvard Center for Neurodegeneration and Repair, Harvard Medical School.

REFERENCES

1. Wong MS, Mak AF, Luk KD, Evans JH, Brown B. Effectiveness and biomechanics of spinal orthoses in the treatment of adolescent idiopathic scoliosis (AIS). Prosthet Orthot Int 2000;24:148–162. [PubMed: 11061202]
2. Nachemson AL, Peterson LE. Effectiveness of treatment with a brace in girls who have adolescent idiopathic scoliosis. A prospective, controlled study based on data from the Brace Study of the Scoliosis Research Society. J Bone Joint Surg Am 1995;77:815–822. [PubMed: 7782353]
3. Winter, RB.; Denis, F.; Lonstein, JE.; Garamella, J.; Lonstein, JE.; Moe, JH. Moe's textbook of scoliosis and other spinal deformities. WB Saunders; Philadelphia: 1995. Techniques of surgery.; p. 133-218.
4. Kitahara H, Inoue S, Minami S, Isobe K, Ohtsuka Y. Long-term results of spinal instrumentation surgery for scoliosis five years or more after surgery, in patients over twenty-three years of age. Spine 1989;14:744–749. [PubMed: 2772726]
5. Adler N, Bleck EE, Rinsky LA, Young W. Balance reactions and eye-hand coordination in idiopathic scoliosis. J Orthop Res 1986;4:102–107. [PubMed: 3950801]
6. Byl NN, Gray JM. Complex balance reactions in different sensory conditions: adolescents with and without idiopathic scoliosis. J Orthop Res 1993;11:215–227. [PubMed: 8483034]
7. Byl NN, Holland S, Jurek A, Hu SS. Postural imbalance and vibratory sensitivity in patients with idiopathic scoliosis: implications for treatment. J Orthop Sports Phys Ther 1997;26:60–68. [PubMed: 9243403]
8. O'Beirne J, Goldberg C, Dowling FE, Fogarty EE. Equilibrial dysfunction in scoliosis—cause or effect? J Spinal Disord 1989;2:184–189. [PubMed: 2520074]
9. Sahlstrand T, Petruson B. A study of labyrinthine function in patients with adolescent idiopathic scoliosis. I. An electro-nystagmographic study. Acta Orthop Scand 1979;50:759–769. [PubMed: 534551]
10. Sahlstrand T, Petruson B, Ortengren R. Vestibulospinal reflex activity in patients with adolescent idiopathic scoliosis. Postural effects during caloric labyrinthine stimulation recorded by stabilometry. Acta Orthop Scand 1979;50:275–281. [PubMed: 314221]
11. Zadeh HG, Sakka SA, Powell MP, Mehta MH. Absent superficial abdominal reflexes in children with scoliosis. An early indicator of syringomyelia. J Bone Joint Surg Br 1995;77:762–767. [PubMed: 7559706]
12. Yekutiel M, Robin GC, Yarom R. Proprioceptive function in children with adolescent idiopathic scoliosis. Spine 1981;6:560–566. [PubMed: 7336278]
13. Cheng JCY, Guo X, Sher AH. Posterior tibial nerve somatosensory cortical evoked potentials in adolescent idiopathic scoliosis. Spine 1998;23:332–337. [PubMed: 9507621]
14. Cheng JCY, Guo X, Sher AH, Chan YL, Metreweli C. Correlation between curve severity, somatosensory evoked potentials, and magnetic resonance imaging in adolescent idiopathic scoliosis. Spine 1999;24:1679–1684. [PubMed: 10472102]
15. Hausmann ON, Boni T, Pfirrmann CW, Curt A, Min K. Preoperative radiological and electrophysiological evaluation in 100 adolescent idiopathic scoliosis patients. Eur Spine J 2003;12:501–506. [PubMed: 12905054]

16. Guo X, Chau WW, Hui-Chan CW, Cheung CS, Tsang WW, Cheng JC. Balance control in adolescents with idiopathic scoliosis and disturbed somatosensory function. Spine 2006;31:E437–E440. [PubMed: 16778672]

17. Gauchard GC, Lascombes P, Kuhnast M, Perrin PP. Influence of different types of progressive idiopathic scoliosis on static and dynamic postural control. Spine 2001;26:1052–1058. [PubMed: 11337624]

18. Cheng JCY, Chau WW, Guo X, Chan YL. Redefining the magnetic resonance imaging reference level for the cerebellar tonsil: a study of 170 adolescents with normal versus idiopathic scoliosis. Spine 2003;28:815–818. [PubMed: 12698126]

19. Chu WC, Lam WW, Chan YL, et al. Relative shortening and functional tethering of spinal cord in adolescent idiopathic scoliosis?: study with multiplanar reformat magnetic resonance imaging and somatosensory evoked potential. Spine 2006;31:E19–E25. [PubMed: 16395162]

20. Inoue M, Minami S, Nakata Y, et al. Preoperative MRI analysis of patients with idiopathic scoliosis: a prospective study. Spine 2005;30:108–114. [PubMed: 15626990]

21. Liu T, Shen D, Davatzikos C. Deformable registration of cortical structures via hybrid volumetric and surface warping. Neuroimage 2004;22:1790–1801. [PubMed: 15275935]

22. Liu T, Young G, Huang L, Chen NK, Wong ST. 76-space analysis of grey matter diffusivity: methods and applications. Neuroimage 2006;31:51–65. [PubMed: 16434215]

23. Shen D, Davatzikos C. HAMMER: hierarchical attribute matching mechanism for elastic registration. IEEE Transactions on Medical Imaging 2002;21:1421–1439. [PubMed: 12575879]

24. Talairach, J.; Tournoux, P. Co-planar stereotaxic atlas of the human brain. Thieme; New York: 1988.

25. Zhang Y, Brady M, Smith S. Segmentation of brain MR images through a hidden Markov random field model and the expectation-maximization algorithm. IEEE Trans Med Imaging 2001;20:45–57. [PubMed: 11293691]

26. Whitwell JL, Crum WR, Watt HC, Fox NC. Normalization of cerebral volumes by use of intracranial volume: implications for longitudinal quantitative MR imaging. AJNR. Am J Neuroradiol 2001;22:1483–1489. [PubMed: 11559495]

27. Herman R, Mixon J, Fisher A, Maulucci R, Stuyck J. Idiopathic scoliosis and the central nervous system: a motor control problem. The Harrington lecture, 1983. Scoliosis Research Society. Spine 1985;10:1–14. [PubMed: 3885413]

28. Simoneau M, Richer N, Mercier P, Allard P, Teasdale N. Sensory deprivation and balance control in idiopathic scoliosis adolescent. Exp Brain Res 2006;170:576–582. [PubMed: 16307257]

29. Yamada K, Yamamoto H, Nakagawa Y, Tezuka A, Tamura T, Kawata S. Etiology of idiopathic scoliosis. Clin Orthop Relat Res 1984:50–57. [PubMed: 6705364]

30. Wiener-Vacher SR, Mazda K. Asymmetric otolith vestibulo-ocular responses in children with idiopathic scoliosis. J Pediatr 1998;132:1028–1032. [PubMed: 9627598]

31. Chau, WW.; Guo, X.; Fu, LL., et al. Abnormal somatosensory evoked potential (SSEP) in adolescent with idiopathic scoliosis - the site of abnormality.. In: Sawatzky, BJ., editor. International Research Society of Spinal Deformities Symposium 2004; Vancouver, Canada. 2004; p. 279-281.

32. Lowe TG, Edgar M, Margulies JY, et al. Etiology of idiopathic scoliosis: current trends in research. J Bone Joint Surg Am 2000;82:1157–1168. [PubMed: 10954107]

33. Burwell RG, Freeman BJ, Dangerfield PH, et al. Left-right upper arm length asymmetry associated with apical vertebral rotation in subjects with thoracic scoliosis: anomaly of bilateral symmetry affecting vertebral, costal and upper arm physes? Stud Health Technol Inform 2006;123:66–71. [PubMed: 17108405]

34. Burwell RG, Aujla RK, Freeman BJ, et al. Patterns of extra-spinal left-right skeletal asymmetries and proximo-distal disproportion in adolescent girls with lower spine scoliosis: ilio-femoral length asymmetry & bilateral tibial/foot length disproportion. Stud Health Technol Inform 2006;123:101–108. [PubMed: 17108411]

35. Adams, RD.; Victor, M.; Ropper, AH. Disorders of motility.. In: Adams, RD.; Victor, M.; Ropper, AH., editors. Principles of neurology. McGraw-Hill; New York: 1997. p. 64-83.

36. Murray EA, Richmond BJ. Role of perirhinal cortex in object perception, memory, and associations. Curr Opin Neurobiol 2001;11:188–193. [PubMed: 11301238]

37. Barrios C, Arrotegui JI. Experimental kyphoscoliosis induced in rats by selective brain stem damage. Int Orthop 1992;16:146–151. [PubMed: 1428313]

38. Hamanishi C, Tanaka S, Kasahara Y, Shikata J. Progressive scoliosis associated with lateral gaze palsy. Spine 1993;18:2545–2548. [PubMed: 8303464]

39. Davatzikos C. Why voxel-based morphometric analysis should be used with great caution when characterizing group differences. Neuroimage 2004;23:17–20. [PubMed: 15325347]

40. Ashburner J, Friston KJ. Voxel-based morphometry - the methods. Neuroimage 2000;11:805–821. [PubMed: 10860804]

41. Counsell SJ, Dyet LE, Larkman DJ, et al. Thalamo-cortical connectivity in children born preterm mapped using probabilistic magnetic resonance tractography. Neuroimage 2007;34:896–904. [PubMed: 17174575]

42. Cherubini A, Luccichenti G, Fasano F, et al. Imaging nervous pathways with MR tractography. Radiol Med (Torino) 2006;111:268–283. [PubMed: 16671384]

43. Bammer R, Acar B, Moseley ME. In vivo MR tractography using diffusion imaging. Eur J Radiol 2003;45:223–234. [PubMed: 12595107]

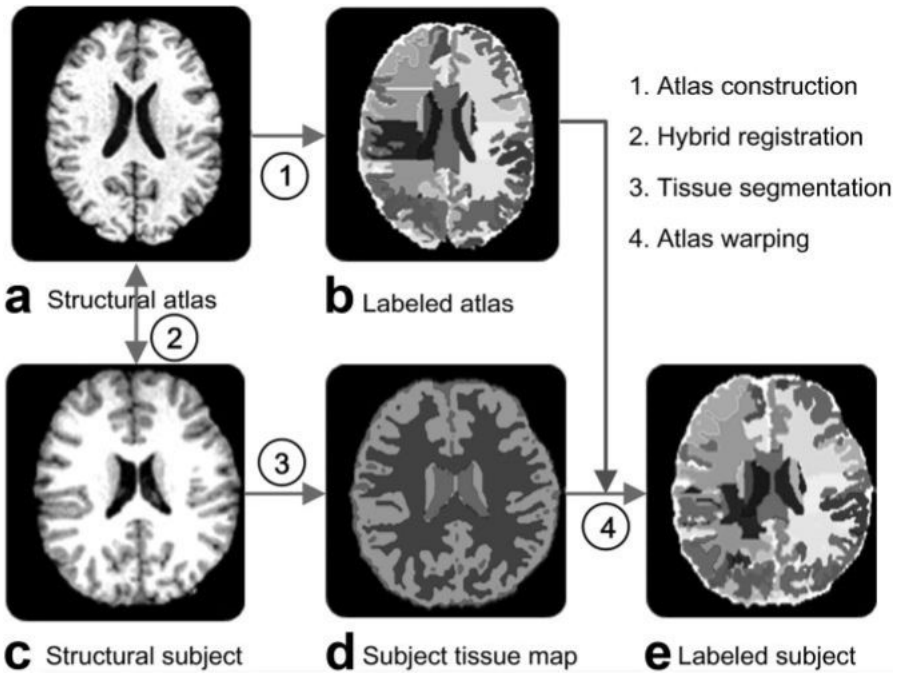

Figure 1.

a–e: Brain images of an adolescent idiopathic scoliosis (AIS) subject illustrating the procedure for automatic parcellation of the whole brain into 99 regions. In (d), the light gray, dark gray, and white colors represent cerebrospinal fluid, white matter, and gray matter, respectively. The colors in b and e are randomly selected to represent the 99 neuroanatomic regions. These regions are much better appreciated on the original image analysis program and might not be fully represented in this gray-scale picture.

Table 1

Summary of 22 of 99 Anatomical Regions That Show Significant Difference on Normalized Mean Regional Brain Volume Between AIS Subjects and Matched Controls With $P \leq 0.01$ Based on Analysis of Variance Test

Brain region	Relationship to normal controls	Normalized ratio in AIS	Normalized ratio in controls	*P* values (2-tailed)
L superior frontal gyrus	Larger	0.00698	0.00553	0.002
L medial frontal gyrus	Larger	0.00837	0.00734	0.010
L lateral fronto-orbital gyrus	Larger	0.10082	0.00838	<0.001
L postcentral gyrus	Larger	0.00800	0.00648	0.003
L thalamus	Larger	0.00474	0.00366	0.007
L frontal lobe white matter	Larger	0.61622	0.52719	0.004
L parietal lobe white matter	Larger	0.31811	0.26265	0.002
L temporal lobe white matter	Larger	0.41556	0.33505	<0.001
L hippocampus	Smaller	0.00169	0.00252	0.002
R anterior limb, internal capsule	Smaller	0.00172	0.00230	0.007
R posterior limb, internal capsule and cerebral peduncle	Smaller	0.00106	0.00151	0.001
R caudate nucleus	Smaller	0.00142	0.00185	0.005
Right temporal pole	Smaller	0.00264	0.00455	<0.001
L inferior occipital gyrus	Smaller	0.00213	0.00308	0.003
L middle occipital gyrus	Smaller	0.00207	0.00314	<0.001
L amygdala	Smaller	0.00032	0.00053	<0.001
R perirhinal	Smaller	0.00104	0.00198	<0.001
L perirhinal	Smaller	0.00082	0.00163	<0.001
R precuneus	Smaller	0.00173	0.00212	0.010
L precuneus	Smaller	0.00145	0.00200	0.002
Corpus callosum	Larger	0.00761	0.00563	<0.001
Brainstem	Larger	0.20844	0.17874	0.005

AIS, adolescent idiopathic scoliosis; L, left; R, right.